



## Synthesis, biological evaluation, and molecular docking studies of resveratrol derivatives possessing chalcone moiety as potential antitubulin agents

Ban-Feng Ruan<sup>a</sup>, Xiang Lu<sup>a</sup>, Jian-Feng Tang<sup>a</sup>, Yao Wei<sup>a</sup>, Xiao-Liang Wang<sup>a</sup>, Yan-Bin Zhang<sup>a</sup>, Li-Sheng Wang<sup>b</sup>, Hai-Liang Zhu<sup>a,\*</sup>

<sup>a</sup> State Key Laboratory of Pharmaceutical Biotechnology, Nanjing University, Nanjing 210093, PR China

<sup>b</sup> School of Chemistry and Chemical Engineering, Guangxi University, Nanning 530004, PR China

### ARTICLE INFO

#### Article history:

Received 2 January 2011

Revised 26 February 2011

Accepted 1 March 2011

Available online 5 March 2011

#### Keywords:

Resveratrol

Chalcone

Antiproliferative activity

Molecular docking

Antitubulin polymerization

### ABSTRACT

Twenty-three resveratrol derivatives possessing chalcone moiety were synthesized and characterized, and their biological activities were also evaluated as potential antiproliferation and tubulin polymerization inhibitors. Compound **C19** exhibited the most potent activity in vitro, which inhibited the growth of HepG2, B16-F10, and A549 cell lines with IC<sub>50</sub> values of 0.2, 0.1, and 1.4 μg/mL, respectively. Compound **C19** also exhibited significant tubulin polymerization inhibitory activity (IC<sub>50</sub> = 2.6 μg/mL). Docking simulation was performed to position compound **C19** into the tubulin–colchicine binding site to determine the probable binding mode.

© 2011 Published by Elsevier Ltd.

### 1. Introduction

Resveratrol, a naturally occurring phytoalexin (3,5,4'-*trans*-trihydroxy-stilbene) present in medicinal plants, grape skin, peanuts, and red wine,<sup>1</sup> has been reported to have chemopreventive activity,<sup>2</sup> by exerting antiproliferative and proapoptotic effects in human cancer cells at all stages of carcinogenesis: initiation, promotion, and progression.<sup>3</sup> These effects are mediated through several biological receptors, including cyclooxygenase (COX),<sup>4</sup> lipoxygenase (LOX),<sup>5</sup> nuclear factor kappa-light-chain-enhancer of activated B cells (NF-κB),<sup>6</sup> quinone reductase 2 (QR2),<sup>7,8</sup> ornithine decarboxylase (ODC),<sup>9</sup> and aromatase.<sup>10</sup>

Chalcones (1,3-diaryl-2-propen-1-ones) are flavonoids and isoflavonoids precursors which are abundant in edible plants and display a wide variety of anticancer,<sup>11–13</sup> anti-inflammatory,<sup>14,15</sup> anti-invasive,<sup>16</sup> antituberculosis,<sup>17</sup> and antifungal activities.<sup>18</sup> Their wide-range biological properties are largely attributed to the α,β-unsaturated ketone moiety. Introduction of various substituents into the two aryl rings is also a field of interest to screen pharmacologically active chalcones.<sup>19</sup>

The microtubule system of eukaryotic cells is an important target for development of antitumor agents. Antimitotic agents cause

mitotic arrest in eukaryotic cells by interfering with the normal microtubule polymerization/depolymerization process. Classic antimitotic agents, many of which are tubulin-binding agents, such as taxanes<sup>20</sup> and vinca alkaloids,<sup>21</sup> interfere with microtubule dynamics by targeting tubulin and are widely used to treat human cancers. However, neurotoxicity, difficult synthesis, and development of multidrug resistance, mainly through the expression of P-glycoprotein (Pgp), have limited their clinical use. Therefore, it is important to develop new tubulin-binding agents or other antimitotic agents with novel modes of action. Among them, Combretastatin A-4 (CA-4, **1**) is a structurally very simple natural product with potent cytotoxic activity.<sup>22</sup> The mechanism of action of CA-4 involves reversible, high affinity binding in the colchicine site of tubulin. As a result of the relatively simple chemical structure and unique biological profiles, CA-4 has stimulated a lot of research in the last two decades<sup>23</sup> (Fig. 1).

Herein we report the synthesis and bioactivities of a series of novel resveratrol derivatives possessing chalcone moiety to mimic the reported antimitotic agents. Their antiproliferative and inhibition of tubulin polymerization activities were evaluated. Molecular modeling studies were consequently performed to understand tubulin–inhibitor interaction. The docking results confirmed that the combination of static and hydrophobic interactions and hydrogen bonding may contribute to the potent biological activities.

\* Corresponding author. Tel.: +86 25 83592672.

E-mail address: [zhuhl@nju.edu.cn](mailto:zhuhl@nju.edu.cn) (H.-L. Zhu).

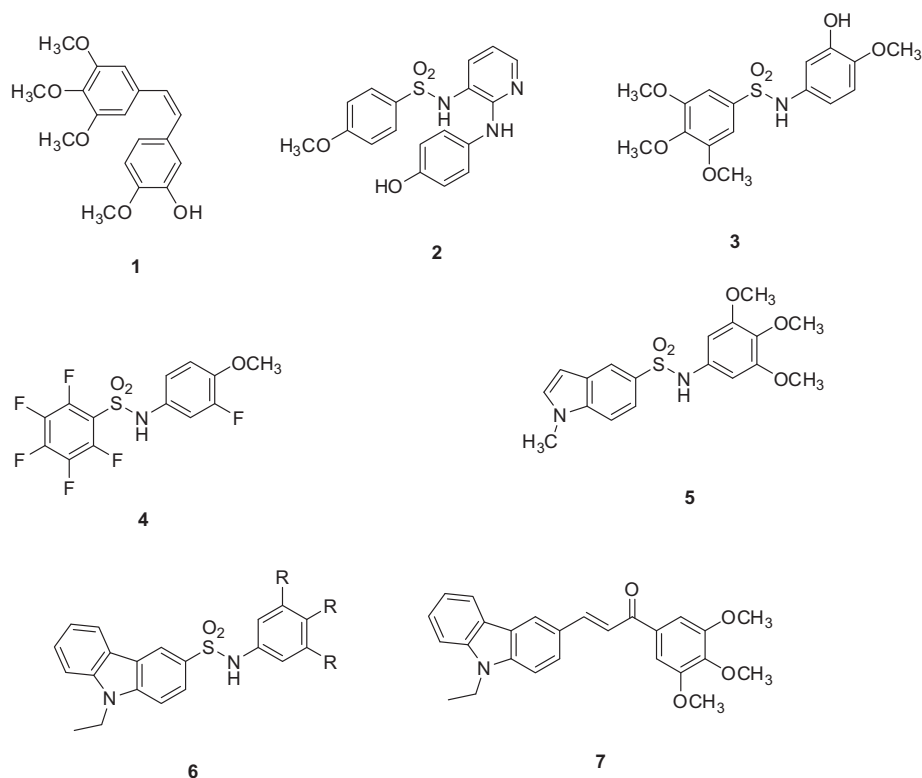
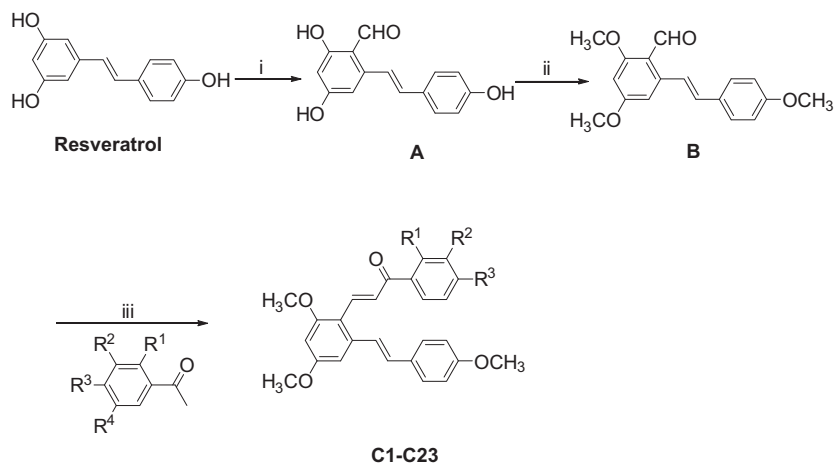


Figure 1. Lead compound and antimitotic agents.



Scheme 1. Synthesis of compounds **C1–C23**. Reagents and conditions: (i)  $\text{CH}_3\text{CN}$ , DMF,  $\text{POCl}_3$ ; (ii)  $\text{CH}_3\text{COCH}_3$ ,  $\text{CH}_3\text{I}$ , reflux, 24 h; (iii)  $\text{CH}_3\text{CH}_2\text{OH}$ , 40% NaOH, 24 h.

## 2. Results and discussion

### 2.1. Chemistry

The synthesis of compounds **C1–C23** is outlined in Scheme 1. The synthesis of these compounds started from resveratrol. The key intermediate, (*E*)-2,4-dimethoxy-6-(4-methoxystyryl)benzaldehyde (**B**), was prepared in two steps as previously reported with some modification.<sup>24,25</sup>

First, (*E*)-2,4-dihydroxy-6-(4-hydroxystyryl)benzaldehyde (**A**) was prepared by the Vilsmeier reaction in  $\text{CH}_3\text{CN}$  from resveratrol in a high yield (98%). The desired intermediate (**B**) was obtained by

reaction of (**A**) with  $\text{CH}_3\text{I}$  in acetone/ $\text{K}_2\text{CO}_3$  under refluxing. The synthesis of the target compounds **C1–C23** were prepared by the Claisen–Schmidt condensation between (**B**) and a series of ketones in the presence of 40% KOH in ethanol<sup>26</sup> in 82–90% yields. All the synthetic compounds were characterized by  $^1\text{H}$  NMR, elemental analysis and mass spectrum, which were in full accordance with their depicted structures.

### 2.2. Biological activity

All the synthesized compounds **C1–C23** were evaluated for their antiproliferative activities against human HepG2 hepatoma cells,

**Table 1**  
Inhibition (IC<sub>50</sub>) of HepG2, B16-F10 and A549 cells proliferation and inhibition of tubulin polymerization by compounds **C1–C23**

Compound	IC <sub>50</sub> ± SD (µg/mL)			
	HepG2 <sup>a</sup>	B16-F10 <sup>a</sup>	A549 <sup>a</sup>	Tubulin <sup>b</sup>
<b>C1</b>	6.8 ± 0.3	3.7 ± 0.2	3.9 ± 0.4	34 ± 2
<b>C2</b>	11.6 ± 2	4.3 ± 0.7	6.1 ± 0.6	59 ± 10
<b>C3</b>	4.9 ± 0.3	5.8 ± 0.1	4.5 ± 0.3	43 ± 10
<b>C4</b>	8.0 ± 0.25	6.4 ± 0.2	7.5 ± 0.4	26 ± 5
<b>C5</b>	12.9 ± 6	5.3 ± 0.13	8.7 ± 0.36	94 ± 9
<b>C6</b>	11.1 ± 4	6.7 ± 0.14	9.4 ± 0.6	55 ± 4
<b>C7</b>	16.2 ± 4	10.4 ± 4	8.4 ± 0.5	131 ± 16
<b>C8</b>	11.6 ± 6	12.7 ± 6	7.9 ± 0.45	58 ± 6
<b>C9</b>	12.2 ± 2	5.3 ± 0.2	6.6 ± 0.3	64 ± 3
<b>C10</b>	13.6 ± 2	4.9 ± 0.12	6.4 ± 0.25	80 ± 13
<b>C11</b>	12.9 ± 8	6.5 ± 0.18	8.3 ± 0.6	72 ± 8
<b>C12</b>	9.5 ± 0.8	3.3 ± 0.19	5.6 ± 0.23	41 ± 2
<b>C13</b>	13.0 ± 3	5.1 ± 0.24	8.1 ± 0.7	76 ± 4
<b>C14</b>	10.8 ± 2	7.5 ± 0.4	5.9 ± 0.6	47 ± 1
<b>C15</b>	18.7 ± 7	4.3 ± 0.24	7.8 ± 0.42	150 ± 15
<b>C16</b>	4.8 ± 0.15	5.3 ± 0.3	3.6 ± 0.14	29 ± 2
<b>C17</b>	5.3 ± 4	6.1 ± 0.32	5.9 ± 0.25	42 ± 6
<b>C18</b>	0.9 ± 0.15	4.0 ± 0.1	0.3 ± 0.11	4.1 ± 0.4
<b>C19</b>	0.2 ± 0.01	1.4 ± 0.08	0.1 ± 0.15	2.6 ± 0.6
<b>C20</b>	7.5 ± 0.7	2.8 ± 0.15	3.8 ± 0.12	36 ± 9
<b>C21</b>	6.3 ± 0.5	8.1 ± 0.4	5.4 ± 0.28	33 ± 4
<b>C22</b>	10.5 ± 3	10.6 ± 4	4.6 ± 0.36	44 ± 5
<b>C23</b>	7.3 ± 0.2	3.3 ± 0.25	3.8 ± 0.2	38 ± 4
RES	38.9 ± 6	37.3 ± 3	30.4 ± 4	158 ± 20
Colchicine	0.23 ± 0.02	0.5 ± 0.04	0.12 ± 0.01	1.3 ± 0.4
CA-4	0.019 ± 0.04	0.4 ± 0.15	0.09 ± 0.01	0.70 ± 0.2

<sup>a</sup> Inhibition of the growth of tumor cell lines.

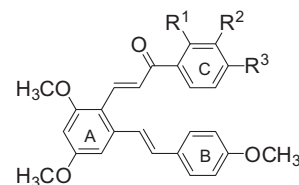
<sup>b</sup> Inhibition of tubulin polymerization.

melanoma B16-F10 cells, and human non-small cell lung cancer A549 cells. The results were summarized in Table 1.

For all the studied compounds, we can see that the antiproliferative activities against HepG2, B16-F10, and A549 cells are, in general, much better than resveratrol. Among them, the oxyalkyl derivatives **C2–C8** showed almost the same moderate antiproliferative activities with 2 to 10-fold higher IC<sub>50</sub> values than that of resveratrol and it also can be observed that the length of the oxyalkyl chain affected little on the antiproliferative activities of **C2–C8**; The alkylated resveratrol analogues **C16–C19**, especially **C19** displayed the most potent inhibitory activity (IC<sub>50</sub> = 0.2 µg/mL for HepG2, 1.4 µg/mL for B16-F10, and 0.1 µg/mL for A549), compared to the positive control. However, structure-relationships in this series of resveratrol derivatives that possessing chalcone moiety demonstrated that there was just a slight difference between the antiproliferative activities against HepG2, B16-F10, and A549 cells of all the studied compounds except **C18** and **C19**, indicating that substituted groups on the C-ring (Fig. 2) may not play a key role in the antiproliferative activities and the existence of resveratrol skeleton together with the chalcone moiety might be responsible for the antiproliferative activities.

To examine whether the compounds interact with tubulin and inhibit tubulin polymerization in vitro, we performed the tubulin assembly assay in a cell-free immunoassay system. The inhibition of tubulin polymerization by resveratrol derivatives were shown in Table 1. Compound **C19** showed the most potent inhibitory effect and its 50% tubulin polymerization inhibition was 2.6 µg/mL.

Furthermore, cell cycle analysis of compound **C19** was performed using flow cytometry, see Figure 3. It can be seen that compound **C19** strongly induced G2/M arrest in B16-F10 cells, and the effect was observed in a dose-independent manner after treatment for 24 h increasing amounts of this compound. About 31.5% of the cells were arrested in the G2/M phase while 72.1% of the cells were found to be in the G2/M phase in the presence of 1 and 5 µg/mL **C19**, respectively. These findings indicated a continuing impair-



C1-C23	R <sup>1</sup> R <sup>2</sup> R <sup>3</sup>		
	R <sup>1</sup>	R <sup>2</sup>	R <sup>3</sup>
<b>C1</b>	H	H	H
<b>C2</b>	H	OCH <sub>3</sub>	H
<b>C3</b>	H	H	OCH <sub>3</sub>
<b>C4</b>	H	H	OCH <sub>2</sub> CH <sub>3</sub>
<b>C5</b>	H	H	O(CH <sub>2</sub> ) <sub>3</sub> CH <sub>3</sub>
<b>C6</b>	H	H	OCH(CH <sub>3</sub> )(CH <sub>2</sub> ) <sub>2</sub> CH <sub>3</sub>
<b>C7</b>	H	H	O(CH <sub>2</sub> ) <sub>5</sub> CH <sub>3</sub>
<b>C8</b>	H	H	O(CH <sub>2</sub> ) <sub>11</sub> CH <sub>3</sub>
<b>C9</b>	H	H	F
<b>C10</b>	H	H	Cl
<b>C11</b>	H	H	Br
<b>C12</b>	H	Cl	H
<b>C13</b>	H	Br	H
<b>C14</b>	H	Cl	Cl
<b>C15</b>	H	H	CF <sub>3</sub>
<b>C16</b>	H	H	CH <sub>3</sub>
<b>C17</b>	CH <sub>3</sub>	H	H
<b>C18</b>	CH <sub>3</sub>	H	CH <sub>3</sub>
<b>C19</b>	H	CH <sub>3</sub>	CH <sub>3</sub>
<b>C20</b>	H	H	NH <sub>2</sub>
<b>C21</b>	H	H	N(CH <sub>2</sub> CH <sub>3</sub> ) <sub>2</sub>
<b>C22</b>	H	H	
<b>C23</b>	H	H	

**Figure 2.** Chemical structures of compounds **C1–C23**.

ment of cell division and confirmed compound **C19** was a potent antitubulin agent.

To gain better understanding on the potency of the studied compounds and guide further SAR studies, we proceeded to examine the interaction of compound **C19** with tubulin (PDB code: 1SA0). The molecular docking was performed by simulation of compound **C19** into the colchicine binding site of tubulin. All docking runs were applied the Lamarckian genetic algorithm of Auto-Dock 4.0. The binding modes of compound **C19** and tubulin were depicted in Figure 4. All the amino acid residues which had interactions with tubulin were exhibited. In the binding mode, compound **C19** is nicely bound to the colchicine binding site of tubulin via hydrophobic interactions and binding is stabilized by two hydrogen bonds. The oxygen atom of the  $\alpha,\beta$ -unsaturated carbonyl system formed one hydrogen bond with the amino hydrogen of Ser 178 (bond length: Ser178 N–H...O = 1.971 Å; bond angle: Ser178 N–H...O = 129.5°) and the oxygen atom of one of the methoxyl groups on A-ring of **C19** formed another one with the amino hydrogen of Val 355 (bond length: Val355 N–H...O = 2.044 Å; bond angle: Val355 N–H...O = 135.5°). The 3D model of the interaction between **C19** and the colchicine binding site was depicted in Figure 5, showing well binding affinity to the target. We can clearly see that the hydrophobic pockets of colchicine binding site are occupied by a methoxy group on A ring and the carboxyl group of the  $\alpha,\beta$ -unsaturated ketone moiety. The two methyl groups on the C-ring may play an auxiliary role in stabilizing the interaction between **C19** and the colchicine binding site. The results of the molecular docking study showed that the resveratrol skeleton and the  $\alpha,\beta$ -unsaturated carbonyl system of the chalcone could act synergistically to interact with the colchicine binding site of tubulin, suggesting that compound **C19** is a potential inhibitor of tubulin.

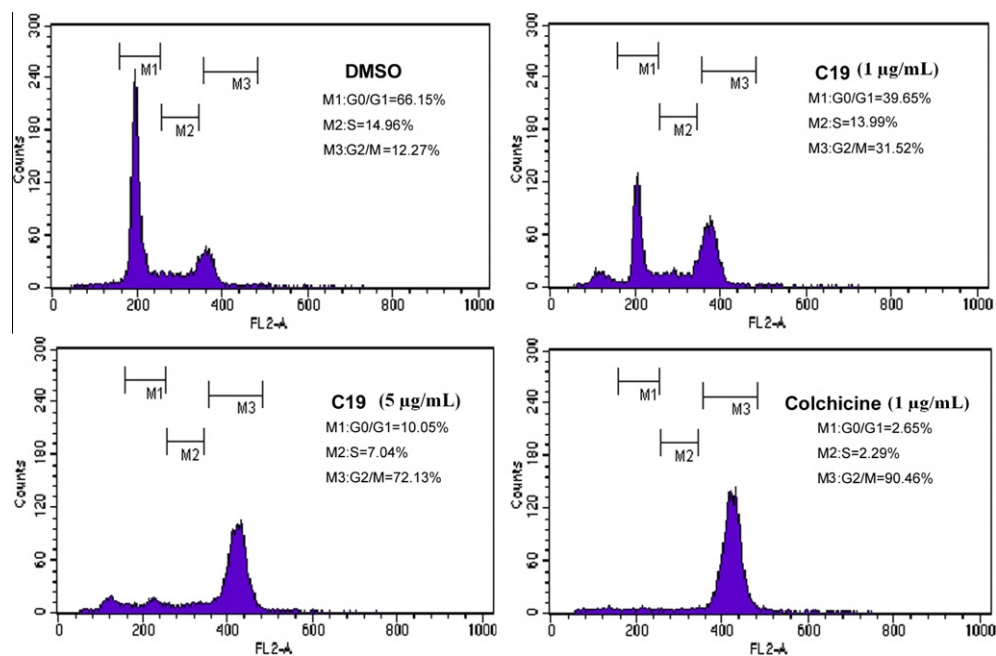


**Figure 3.** Effects of compound **C19** on cell cycle progression of B16-F10 cells were determined by flow cytometry analysis. B16-F10 cells were treated with different concentrations of **C19** for 24 h. The percentage of cells in each cycle phase was indicated.

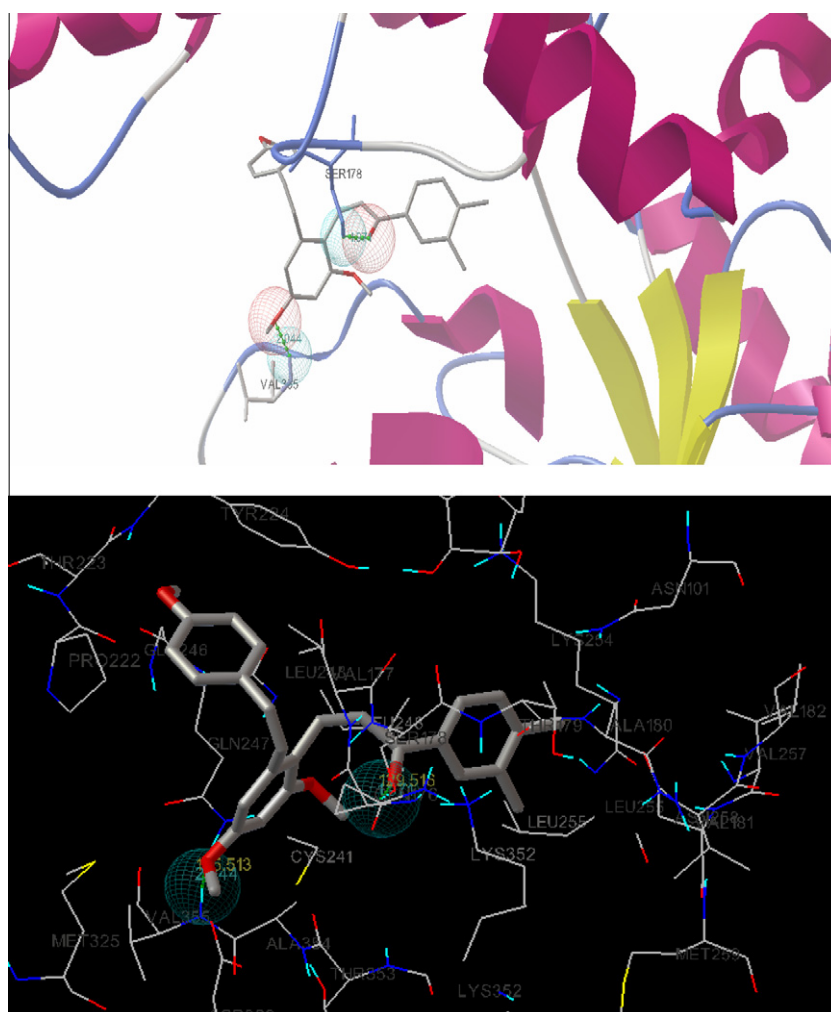


**Figure 4.** Compound **C19** (colored by atom: carbons: gray; oxygens: red) is bond into tubulin (entry 1SA0 in the Protein Data Bank). The dotted lines show the hydrogen bonds.

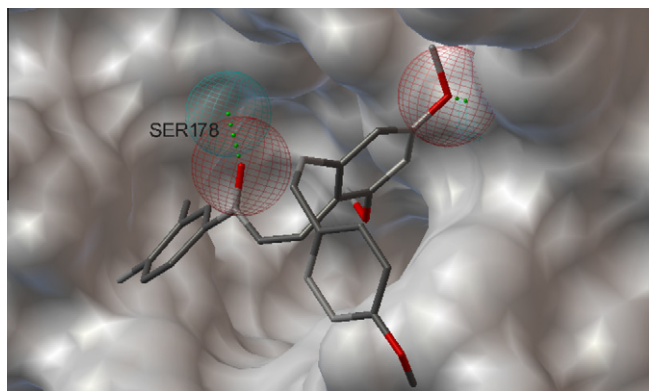


**Figure 5.** The surface model structure of **C19**–tubulin complex. The dotted lines show the hydrogen bonds.

### 3. Conclusions

In our present work, a series of novel antitubulin polymerization inhibitors (**C1**–**C23**) containing resveratrol skeleton and chalcone moiety had been synthesized and evaluated. These compounds exhibited potent tubulin polymerization inhibitory activity and antiproliferative activities against HepG2, B16-F10, and A549 tumor cell lines. Compound **C19** showed the most potent activity which inhibited the growth of HepG2, B16-F10, and A549 cell lines with  $IC_{50}$  values of  $0.2 \pm 0.01$ ,  $1.4 \pm 0.08$ , and  $0.1 \pm 0.15$   $\mu\text{g}/\text{mL}$  and inhibited the polymerization of tubulin with  $IC_{50}$  of  $2.6 \pm 0.6$   $\mu\text{g}/\text{mL}$ . Molecular docking was performed to study the inhibitor-tubulin protein interactions. Analysis of the binding conformation of compound **C19** in the colchicine binding site demonstrated that several interactions with the protein residues led to the antitubulin polymerization and antiproliferative activity.

### 4. Experimental

#### 4.1. Chemistry

All the NMR spectra were recorded on a Bruker DRX 400 or DPX 300 model Spectrometer in  $\text{CDCl}_3$ . Chemical shifts ( $\delta$ ) for  $^1\text{H}$  NMR spectra were reported in parts per million to residual solvent protons. Melting points were measured on a Boetius micro melting point apparatus. The ESI-MS spectra were recorded on a Mariner System 5304 Mass spectrometer. Carbon, hydrogen, and nitrogen assays were carried out with a CHN–O–Rapid instrument and were within  $\pm 0.4\%$  of the theoretical values. TLC was run on the silica gel coated aluminum sheets (Silica Gel 60 GF254, E. Merk, Germany) and visualized in UV light (254 nm).

#### 4.2. Synthesis method for (*E*)-2,4-dihydroxy-6-(4-hydroxystyryl)benzaldehyde (**A**)

To a solution of resveratrol (2.28 g, 0.01 mol) in 50 mL of  $\text{CH}_3\text{CN}$  and DMF (0.73 g, 0.01 mol),  $\text{POCl}_3$  (2.30 g, 0.015 mol) was added dropwise while cooling with an ice/water bath for 0.5 h. The reaction mixture was stirred for another 2 h at room temperature. Then, the solution was added to cold water (300 mL). The yellow solution was stirred under  $50^\circ\text{C}$  for 3 h, and extracted with EtOAc (100 mL  $\times$  3). The combined organic layers were washed with water, dried over anhydrous sodium sulfate, filtered and evaporated. Purification by silica gel afforded (**A**) as yellow powder in 96% yield. Mp:  $210$ – $212^\circ\text{C}$ .  $^1\text{H}$  NMR (DMSO- $d_6$ ): 6.21 (s, 1H), 6.62 (s, 1H), 6.78 (d, 2H,  $J = 8.4$  Hz), 7.02 (d, 1H,  $J = 16.0$  Hz), 7.49 (d, 2H,  $J = 8.4$  Hz), 7.70 (d, 1H,  $J = 16.2$  Hz), 9.71 (s, 1H), 10.27 (s, 1H), 10.76 (s, 1H), 12.12 (s, 1H). MS (ESI): 257.3 ( $\text{C}_{15}\text{H}_{12}\text{O}_4$ ,

$[\text{M}+\text{H}]^+$ ). Anal. Calcd for  $\text{C}_{15}\text{H}_{12}\text{O}_4$ : C, 51.05; H, 3.86. Found: C, 50.91; H, 3.87.

#### 4.3. Synthesis method for (*E*)-2,4-dimethoxy-6-(4-methoxystyryl)benzaldehyde (**B**)

To a solution of **A** (1.28 g, 0.005 mol) and anhydrous  $\text{K}_2\text{CO}_3$  (2.07 g, 0.015 mol) in 10 mL of  $\text{CH}_3\text{COCH}_3$ ,  $\text{CH}_3\text{I}$  (2.84 g, 0.02 mol) was added dropwise. The reaction mixture was refluxed for 24 h. After cooling to room temperature, the reaction mixture was filtered and the filtrate was dried and evaporated. Purification by silica gel afforded (**B**) in 84% yield. Mp:  $108$ – $109^\circ\text{C}$ .  $^1\text{H}$  NMR (DMSO- $d_6$ ): 3.78 (s, 3H), 3.90 (s, 3H), 3.92 (s, 3H), 6.63 (s, 1H), 6.91 (s, 1H), 6.97 (d, 2H,  $J = 7.9$  Hz), 7.21 (d, 1H,  $J = 16.2$  Hz), 7.50 (d, 2H,  $J = 7.9$  Hz), 7.95 (d, 1H,  $J = 16.2$  Hz), 10.41 (s, 1H). MS (ESI): 299.3 ( $\text{C}_{18}\text{H}_{18}\text{O}_4$ ,  $[\text{M}+\text{H}]^+$ ). Anal. Calcd for  $\text{C}_{18}\text{H}_{18}\text{O}_4$ : C, 72.47; H, 6.08. Found: C, 72.69; H, 6.07.

#### 4.4. General method of synthesis of compounds **C1**–**C23**

The chalcones were synthesized by a base catalyzed Claisen-Schmidt condensation reaction of substituted acetophenones and (**B**) (Scheme 1). An EtOH solution of substituted acetophenones (1.0 equiv) and (**B**) (1.0 equiv) was added with 50% KOH (2.5 equiv). The reaction mixture was stirred overnight at room temperature; the pH was adjusted to 3–4 with aq 2 M HCl solution; the precipitate was collected by filtration and purified by recrystallization in EtOH.

##### 4.4.1. (*E*)-3-(2,4-Dimethoxy-6-((*E*)-4-methoxystyryl)phenyl)-1-phenylprop-2-en-1-one (**C1**)

Yellow solid (0.364 g, 91% yield). Mp  $118$ – $120^\circ\text{C}$ .  $^1\text{H}$  NMR (400 MHz,  $\text{CDCl}_3$ )  $\delta$  (ppm): 3.86 (s, 3H), 3.93 (s, 3H), 3.94 (s, 3H), 6.47 (s, 1H), 6.76 (s, 1H), 6.92 (d,  $J = 8.0$ , 2H), 6.97 (d,  $J = 16.0$ , 1H), 7.37 (d,  $J = 16.0$ , 1H), 7.52 (d,  $J = 7.6$ , 1H), 7.43–7.51 (dd, 3H), 7.52 (d,  $J = 7.6$ , 1H), 7.60 (d,  $J = 15.6$ , 1H), 8.00 (d,  $J = 7.2$ , 2H), 8.21 (d,  $J = 15.6$ , 1H). MS (ESI): 401.5 ( $\text{C}_{26}\text{H}_{26}\text{O}_4$ ,  $[\text{M}+\text{H}]^+$ ). Anal. Calcd for  $\text{C}_{26}\text{H}_{26}\text{O}_4$ : C, 78.98; H, 6.04. Found: C, 78.23; H, 6.03.

##### 4.4.2. (*E*)-3-(2,4-Dimethoxy-6-((*E*)-4-methoxystyryl)phenyl)-1-(3-methoxyphenyl)prop-2-en-1-one (**C2**)

Yellow solid (0.353 g, 82% yield). Mp  $94$ – $95^\circ\text{C}$ .  $^1\text{H}$  NMR (400 MHz,  $\text{CDCl}_3$ )  $\delta$  (ppm): 3.83 (s, 3H), 3.86 (s, 3H), 3.93 (s, 6H), 6.47 (s, 1H), 6.76 (s, 1H), 6.92 (d,  $J = 8.4$ , 2H), 6.97 (d,  $J = 16.0$ , 1H), 7.10 (dd, 1H,  $J_1 = 7.6$ ,  $J_2 = 16.4$ ), 7.34 (d,  $J = 16.0$ , 1H), 7.37 (d,  $J = 16.0$ , 1H), 7.49 (d,  $J = 8.4$ , 2H), 7.54 (d,  $J = 8.4$ , 1H), 7.56 (s, 1H), 7.59 (d,  $J = 7.2$ , 1H), 8.21 (d,  $J = 16.0$ , 1H). MS (ESI): 431.2 ( $\text{C}_{27}\text{H}_{26}\text{O}_5$ ,  $[\text{M}+\text{H}]^+$ ). Anal. Calcd for  $\text{C}_{27}\text{H}_{26}\text{O}_5$ : C, 75.33; H, 6.09. Found: C, 75.57; H, 6.08.

##### 4.4.3. (*E*)-3-(2,4-Dimethoxy-6-((*E*)-4-methoxystyryl)phenyl)-1-(4-methoxyphenyl)prop-2-en-1-one (**C3**)

Yellow solid (0.400 g, 92% yield). Mp  $136$ – $138^\circ\text{C}$ .  $^1\text{H}$  NMR (400 MHz,  $\text{CDCl}_3$ )  $\delta$  (ppm):  $^1\text{H}$  NMR (400 MHz,  $\text{CDCl}_3$ )  $\delta$  (ppm): 3.86 (s, 3H), 3.88 (s, 3H), 3.93 (s, 6H), 6.47 (s, 1H), 6.76 (s, 1H), 6.92 (d,  $J = 8.0$ , 4H), 6.97 (d,  $J = 16.0$ , 1H), 7.37 (d,  $J = 16.0$ , 1H), 7.49 (d,  $J = 8.0$ , 2H), 7.58 (d,  $J = 16.0$ , 1H), 8.01 (d,  $J = 8.0$ , 2H), 8.18 (d,  $J = 16.0$ , 1H). MS (ESI): 431.5 ( $\text{C}_{27}\text{H}_{26}\text{O}_5$ ,  $[\text{M}+\text{H}]^+$ ). Anal. Calcd for  $\text{C}_{27}\text{H}_{26}\text{O}_5$ : C, 75.33; H, 6.09. Found: C, 75.13; H, 6.11.

##### 4.4.4. (*E*)-3-(2,4-Dimethoxy-6-((*E*)-4-methoxystyryl)phenyl)-1-(4-ethoxyphenyl)prop-2-en-1-one (**C4**)

Yellow solid (0.360 g, 81% yield). Mp  $131$ – $133^\circ\text{C}$ .  $^1\text{H}$  NMR (400 MHz,  $\text{CDCl}_3$ )  $\delta$  (ppm): 1.46 (t,  $J = 6.8$ , 3H), 3.86 (s, 3H), 3.93 (s, 6H), 4.11 (q,  $J_1 = 14.0$ ,  $J_2 = 7.2$ , 2H), 6.47 (s, 1H), 6.76 (s, 1H), 6.91 (d,  $J = 8.0$ , 4H), 6.97 (d,  $J = 16.0$ , 1H), 7.38 (d,  $J = 16.0$ , 1H),

7.49 (d,  $J = 8.0$ , 2H), 7.58 (d,  $J = 16.0$ , 1H), 7.99 (d,  $J = 8.8$ , 2H), 8.18 (d,  $J = 16.0$ , 1H). MS (ESI): 445.2 ( $C_{28}H_{28}O_5$ ,  $[M+H]^+$ ). Anal. Calcd for  $C_{28}H_{28}O_5$ : C, 75.65; H, 6.35. Found: C, 76.19; H, 6.37.

#### 4.4.5. (E)-1-(4-Butoxyphenyl)-3-(2,4-dimethoxy-6-((E)-4-methoxystyryl)phenyl)prop-2-en-1-one (C5)

Yellow solid (0.369 g, 78% yield). Mp 109–111 °C.  $^1H$  NMR (400 MHz,  $CDCl_3$ )  $\delta$  (ppm): 1.01 (t, 3H,  $J = 7.2$ ), 1.50–1.55 (m, 2H), 1.77–1.84 (m, 2H), 3.86 (s, 3H), 3.93 (s, 6H), 4.04 (t, 2H,  $J = 6.8$ ), 6.47 (s, 1H), 6.76 (s, 1H), 6.92 (d,  $J = 8.0$ , 4H), 6.97 (d,  $J = 16.0$ , 1H), 7.37 (d,  $J = 16.0$ , 1H), 7.49 (d,  $J = 8.0$ , 2H), 7.58 (d,  $J = 16.0$ , 1H), 8.01 (d,  $J = 8.0$ , 2H), 8.18 (d,  $J = 16.0$ , 1H). MS (ESI): 473.2 ( $C_{30}H_{32}O_5$ ,  $[M+H]^+$ ). Anal. Calcd for  $C_{30}H_{32}O_5$ : C, 76.25; H, 6.83. Found: C, 76.51; H, 6.86.

#### 4.4.6. (E)-3-(2,4-Dimethoxy-6-((E)-4-methoxystyryl)phenyl)-1-(4-(pentan-2-yloxy)phenyl)prop-2-en-1-one (C6)

Yellow solid (0.384 g, 79% yield). Mp 76–77 °C.  $^1H$  NMR (400 MHz,  $CDCl_3$ )  $\delta$  (ppm): 0.98 (t, 3H,  $J = 7.2$ ), 1.04 (d, 3H,  $J = 6.8$ ), 1.54–1.65 (m, 4H), 1.86–1.95 (m, 1H), 3.86 (s, 3H), 3.93 (s, 6H), 4.04 (t, 2H,  $J = 6.8$ ), 6.47 (s, 1H), 6.76 (s, 1H), 6.92 (d,  $J = 8.0$ , 4H), 6.97 (d,  $J = 16.0$ , 1H), 7.37 (d,  $J = 16.0$ , 1H), 7.49 (d,  $J = 8.0$ , 2H), 7.58 (d,  $J = 16.0$ , 1H), 8.01 (d,  $J = 8.0$ , 2H), 8.18 (d,  $J = 16.0$ , 1H). MS (ESI): 487.2 ( $C_{31}H_{34}O_5$ ,  $[M+H]^+$ ). Anal. Calcd for  $C_{31}H_{34}O_5$ : C, 76.52; H, 7.04. Found: C, 76.33; H, 7.07.

#### 4.4.7. (E)-3-(2,4-Dimethoxy-6-((E)-4-methoxystyryl)phenyl)-1-(4-(hexyloxy)phenyl)prop-2-en-1-one (C7)

Yellow solid (0.416 g, 83% yield). Mp 99–101 °C.  $^1H$  NMR (400 MHz,  $CDCl_3$ )  $\delta$  (ppm): 0.93 (t, 3H,  $J = 7.2$ ), 1.35–1.38 (m, 4H), 1.47–1.50 (m, 2H), 1.78–1.85 (m, 2H), 3.86 (s, 3H), 3.93 (s, 6H), 4.03 (t, 2H,  $J = 6.8$ ), 6.47 (s, 1H), 6.76 (s, 1H), 6.92 (d,  $J = 8.0$ , 4H), 6.97 (d,  $J = 16.0$ , 1H), 7.37 (d,  $J = 16.0$ , 1H), 7.49 (d,  $J = 8.0$ , 2H), 7.58 (d,  $J = 16.0$ , 1H), 8.01 (d,  $J = 8.0$ , 2H), 8.18 (d,  $J = 16.0$ , 1H). MS (ESI): 501.3 ( $C_{32}H_{36}O_5$ ,  $[M+H]^+$ ). Anal. Calcd for  $C_{32}H_{36}O_5$ : C, 76.77; H, 7.25. Found: C, 76.59; H, 7.28.

#### 4.4.8. (E)-3-(2,4-Dimethoxy-6-((E)-4-methoxystyryl)phenyl)-1-(4-(dodecyloxy)phenyl)prop-2-en-1-one (C8)

Yellow solid (0.415 g, 71% yield). Mp 82–83 °C.  $^1H$  NMR (400 MHz,  $CDCl_3$ )  $\delta$  (ppm): 0.90 (t, 3H,  $J = 7.2$ ), 1.29–1.34 (m, 16H), 1.44–1.51 (m, 2H), 1.78–1.85 (m, 2H), 3.86 (s, 3H), 3.93 (s, 6H), 4.02 (t, 2H,  $J = 6.8$ ), 6.47 (s, 1H), 6.76 (s, 1H), 6.92 (d,  $J = 8.0$ , 4H), 6.97 (d,  $J = 16.0$ , 1H), 7.37 (d,  $J = 16.0$ , 1H), 7.49 (d,  $J = 8.0$ , 2H), 7.58 (d,  $J = 16.0$ , 1H), 8.01 (d,  $J = 8.0$ , 2H), 8.18 (d,  $J = 16.0$ , 1H). MS (ESI): 585.4 ( $C_{38}H_{48}O_5$ ,  $[M+H]^+$ ). Anal. Calcd for  $C_{38}H_{48}O_5$ : C, 78.05; H, 8.27. Found: C, 78.32; H, 8.25.

#### 4.4.9. (E)-3-(2,4-Dimethoxy-6-((E)-4-methoxystyryl)phenyl)-1-(4-fluorophenyl)prop-2-en-1-one (C9)

Yellow solid (0.381 g, 91% yield). Mp 138–140 °C.  $^1H$  NMR (400 MHz,  $CDCl_3$ )  $\delta$  (ppm): 3.87 (s, 3H), 3.93 (s, 3H), 3.94 (s, 3H), 6.47 (s, 1H), 6.76 (s, 1H), 6.93 (d,  $J = 8.0$ , 2H), 6.97 (d,  $J = 16.0$ , 1H), 7.12 (d,  $J = 8.4$ , 2H), 7.36 (d,  $J = 16.0$ , 1H), 7.49 (d,  $J = 8.4$ , 2H), 7.57 (d,  $J = 16.0$ , 1H), 8.02 (d,  $J = 8.4$ , 2H), 8.21 (d,  $J = 16.0$ , 1H). MS (ESI): 419.2 ( $C_{26}H_{23}FO_4$ ,  $[M+H]^+$ ). Anal. Calcd for  $C_{26}H_{23}FO_4$ : C, 74.63; H, 5.54. Found: C, 74.87; H, 5.53.

#### 4.4.10. (E)-1-(4-Chlorophenyl)-3-(2,4-dimethoxy-6-((E)-4-methoxystyryl)phenyl)prop-2-en-1-one (C10)

Yellow solid (0.408 g, 94% yield). Mp 147–149 °C.  $^1H$  NMR (400 MHz,  $CDCl_3$ )  $\delta$  (ppm): 3.87 (s, 3H), 3.93 (s, 3H), 3.94 (s, 3H), 6.47 (s, 1H), 6.76 (s, 1H), 6.93 (d,  $J = 8.0$ , 2H), 6.96 (d,  $J = 16.0$ , 1H), 7.34 (d,  $J = 16.0$ , 1H), 7.42 (d,  $J = 8.4$ , 2H), 7.48 (d,  $J = 8.4$ , 2H), 7.55 (d,  $J = 16.0$ , 1H), 7.93 (d,  $J = 8.4$ , 2H), 8.21 (d,  $J = 15.6$ , 1H).

MS (ESI): 435.1 ( $C_{26}H_{23}ClO_4$ ,  $[M+H]^+$ ). Anal. Calcd for  $C_{26}H_{23}ClO_4$ : C, 71.80; H, 5.33. Found: C, 72.06; H, 5.35.

#### 4.4.11. (E)-1-(4-Bromophenyl)-3-(2,4-dimethoxy-6-((E)-4-methoxystyryl)phenyl)prop-2-en-1-one (C11)

Yellow solid (0.441 g, 92% yield). Mp 159–161 °C.  $^1H$  NMR (400 MHz,  $CDCl_3$ )  $\delta$  (ppm): 3.87 (s, 3H), 3.93 (s, 3H), 3.94 (s, 3H), 6.47 (s, 1H), 6.75 (s, 1H), 6.93 (d,  $J = 8.4$ , 2H), 6.96 (d,  $J = 16.0$ , 1H), 7.34 (d,  $J = 16.0$ , 1H), 7.48 (d,  $J = 8.0$ , 2H), 7.54 (d,  $J = 16.0$ , 1H), 7.58 (d,  $J = 8.4$ , 2H), 7.85 (d,  $J = 8.0$ , 2H), 8.21 (d,  $J = 15.6$ , 1H). MS (ESI): 479.1 ( $C_{26}H_{23}BrO_4$ ,  $[M+H]^+$ ). Anal. Calcd for  $C_{26}H_{23}BrO_4$ : C, 65.14; H, 4.84. Found: C, 65.37; H, 4.86.

#### 4.4.12. (E)-1-(3-Chlorophenyl)-3-(2,4-dimethoxy-6-((E)-4-methoxystyryl)phenyl)prop-2-en-1-one (C12)

Yellow solid (0.331 g, 76% yield). Mp 121–123 °C.  $^1H$  NMR (400 MHz,  $CDCl_3$ )  $\delta$  (ppm): 3.82 (s, 3H), 3.94 (s, 6H), 6.24 (s, 1H), 6.47 (s, 1H), 6.91 (d,  $J = 8.0$ , 2H), 6.92 (d,  $J = 16.0$ , 1H), 7.30 (d,  $J = 8.0$ , 1H), 7.32 (d,  $J = 16.0$ , 1H), 7.44 (d,  $J = 8.0$ , 2H), 7.52 (d,  $J = 16.0$ , 1H), 7.63 (d,  $J = 8.0$ , 1H), 7.82 (dd, 1H, dd, 1H,  $J_1 = 7.6$ ,  $J_2 = 16.4$ ), 8.10 (s, 1H), 8.21 (d,  $J = 16.0$ , 1H). MS (ESI): 435.1 ( $C_{26}H_{23}ClO_4$ ,  $[M+H]^+$ ). Anal. Calcd for  $C_{26}H_{23}ClO_4$ : C, 71.80; H, 5.33. Found: C, 72.04; H, 5.31.

#### 4.4.13. (E)-1-(3-Bromophenyl)-3-(2,4-dimethoxy-6-((E)-4-methoxystyryl)phenyl)prop-2-en-1-one (C13)

Yellow solid (0.431 g, 90% yield). Mp 125–127 °C.  $^1H$  NMR (400 MHz,  $CDCl_3$ )  $\delta$  (ppm): 3.86 (s, 3H), 3.93 (s, 3H), 3.94 (s, 3H), 6.47 (s, 1H), 6.76 (s, 1H), 6.93 (d,  $J = 8.0$ , 2H), 6.96 (d,  $J = 16.0$ , 1H), 7.32 (d,  $J = 8.0$ , 1H), 7.34 (d,  $J = 16.0$ , 1H), 7.49 (d,  $J = 8.0$ , 2H), 7.55 (d,  $J = 16.0$ , 1H), 7.67 (d,  $J = 8.0$ , 1H), 7.86 (dd, 1H,  $J_1 = 7.6$ ,  $J_2 = 16.4$ ), 8.12 (s, 1H), 8.21 (d,  $J = 16.0$ , 1H). MS (ESI): 450.2 ( $C_{26}H_{23}BrO_4$ ,  $[M+H]^+$ ). Anal. Calcd for  $C_{26}H_{23}BrO_4$ : C, 65.14; H, 4.84. Found: C, 64.90; H, 4.86.

#### 4.4.14. (E)-1-(3,4-Dichlorophenyl)-3-(2,4-dimethoxy-6-((E)-4-methoxystyryl)phenyl)prop-2-en-1-one (C14)

Yellow solid (0.404 g, 86% yield). Mp 140–142 °C.  $^1H$  NMR (400 MHz,  $CDCl_3$ )  $\delta$  (ppm): 3.87 (s, 3H), 3.93 (s, 3H), 3.95 (s, 3H), 6.47 (s, 1H), 6.75 (s, 1H), 6.93 (d,  $J = 8.4$ , 2H), 6.96 (d,  $J = 16.0$ , 1H), 7.33 (d,  $J = 15.6$ , 1H), 7.49 (d,  $J = 8.4$ , 3H), 7.53 (d,  $J = 16.0$ , 1H), 7.80 (d,  $J = 8.0$ , 1H), 8.07 (s, 1H), 8.23 (d,  $J = 16.0$ , 1H). MS (ESI): 470.4 ( $C_{26}H_{22}Cl_2O_4$ ,  $[M+H]^+$ ). Anal. Calcd for  $C_{26}H_{22}Cl_2O_4$ : C, 66.53; H, 4.72. Found: C, 66.32; H, 4.70.

#### 4.4.15. (E)-3-(2,4-Dimethoxy-6-((E)-4-methoxystyryl)phenyl)-1-(4-(trifluoromethyl)phenyl)prop-2-en-1-one (C15)

Yellow solid (0.436 g, 93% yield). Mp 178–180 °C.  $^1H$  NMR (400 MHz,  $CDCl_3$ )  $\delta$  (ppm): 3.87 (s, 3H), 3.93 (s, 3H), 3.95 (s, 3H), 6.48 (s, 1H), 6.76 (s, 1H), 6.93 (d,  $J = 8.8$ , 2H), 6.96 (d,  $J = 16.0$ , 1H), 7.34 (d,  $J = 16.0$ , 1H), 7.48 (d,  $J = 8.4$ , 2H), 7.59 (d,  $J = 16.0$ , 1H), 7.70 (d,  $J = 8.0$ , 2H), 8.07 (d,  $J = 8.0$ , 2H), 8.23 (d,  $J = 16.0$ , 1H). MS (ESI): 469.5 ( $C_{27}H_{23}F_3O_4$ ,  $[M+H]^+$ ). Anal. Calcd for  $C_{27}H_{23}F_3O_4$ : C, 69.22; H, 4.95. Found: C, 69.46; H, 4.93.

#### 4.4.16. (E)-3-(2,4-Dimethoxy-6-((E)-4-methoxystyryl)phenyl)-1-(p-tolyl)prop-2-en-1-one (C16)

Yellow solid (0.311 g, 75% yield). Mp 112–114 °C.  $^1H$  NMR (400 MHz,  $CDCl_3$ )  $\delta$  (ppm): 2.43 (s, 3H), 3.86 (s, 3H), 3.93 (s, 6H), 6.47 (s, 1H), 6.76 (s, 1H), 6.92 (d,  $J = 8.8$ , 2H), 6.97 (d,  $J = 16.0$ , 1H), 7.25 (d,  $J = 8.0$ , 2H), 7.38 (d,  $J = 16.0$ , 1H), 7.49 (d,  $J = 8.4$ , 2H), 7.58 (d,  $J = 16.0$ , 1H), 7.91 (d,  $J = 8.0$ , 2H), 8.19 (d,  $J = 16.0$ , 1H). MS (ESI): 415.5 ( $C_{27}H_{26}O_4$ ,  $[M+H]^+$ ). Anal. Calcd for  $C_{27}H_{26}O_4$ : C, 78.24; H, 6.32. Found: C, 78.51; H, 6.34.

**4.4.17. (E)-3-(2,4-Dimethoxy-6-((E)-4-methoxystyryl)phenyl)-1-(o-tolyl)prop-2-en-1-one (C17)**

Yellow solid (0.282 g, 68% yield). Mp 106–108 °C. <sup>1</sup>H NMR (400 MHz, CDCl<sub>3</sub>) δ (ppm): 2.46 (s, 3H), 3.87 (s, 3H), 3.91 (s, 6H), 6.44 (s, 1H), 6.72 (s, 1H), 6.90 (d, *J* = 16.0, 1H), 6.92 (d, *J* = 8.4, 2H), 7.19 (d, *J* = 16.4, 1H), 7.25 (d, *J* = 8.0, 1H), 7.26 (d, *J* = 16.0, 1H), 7.27 (dd, *J* = 8.0, *J*<sub>1</sub> = 7.6, *J*<sub>2</sub> = 15.6, 1H), 7.34 (dd, *J*<sub>1</sub> = 7.6, *J*<sub>2</sub> = 15.6, 1H), 7.39 (d, *J* = 8.4, 2H), 7.50 (d, *J* = 7.6, 1H), 7.86 (d, *J* = 16.0, 1H). MS (ESI): 415.5 (C<sub>27</sub>H<sub>26</sub>O<sub>4</sub>, [M+H]<sup>+</sup>). Anal. Calcd for C<sub>27</sub>H<sub>26</sub>O<sub>4</sub>: C, 78.24; H, 6.32. Found: C, 78.50; H, 6.30.

**4.4.18. (E)-3-(2,4-Dimethoxy-6-((E)-4-methoxystyryl)phenyl)-1-(2,4-dimethylphenyl)prop-2-en-1-one (C18)**

Yellow solid (0.313 g, 73% yield). Mp 112–114 °C. <sup>1</sup>H NMR (400 MHz, CDCl<sub>3</sub>) δ (ppm): 2.36 (s, 3H), 2.46 (s, 3H), 3.86 (s, 3H), 3.92 (s, 3H), 3.95 (s, 3H), 6.41 (s, 1H), 6.78 (s, 1H), 6.92 (d, *J* = 8.0, 3H), 7.00 (d, *J* = 16.4, 1H), 7.02 (s, 1H), 7.22 (d, *J* = 15.6, 1H), 7.41 (d, *J* = 8.4, 1H), 7.53 (d, *J* = 8.4, 2H), 7.88 (d, *J* = 16.0, 1H), 8.08 (d, *J* = 16.0, 1H). MS (ESI): 429.20 (C<sub>28</sub>H<sub>28</sub>O<sub>4</sub>, [M+H]<sup>+</sup>). Anal. Calcd for C<sub>28</sub>H<sub>28</sub>O<sub>4</sub>: C, 78.48; H, 6.59. Found: C, 78.23; H, 6.61.

**4.4.19. (E)-3-(2,4-Dimethoxy-6-((E)-4-methoxystyryl)phenyl)-1-(3,4-dimethylphenyl)prop-2-en-1-one (C19)**

Yellow solid (0.330 g, 77% yield). Mp 111–113 °C. <sup>1</sup>H NMR (400 MHz, CDCl<sub>3</sub>) δ (ppm): 2.36 (s, 3H), 2.46 (s, 3H), 3.79 (s, 3H), 3.89 (s, 3H), 3.93 (s, 3H), 6.63 (s, 1H), 6.84 (s, 1H), 6.97 (d, *J* = 16.0, 1H), 6.99 (d, *J* = 8.4, 2H), 7.09 (d, *J* = 16.0, 1H), 7.37 (d, *J* = 16.0, 1H), 7.56 (s, 1H), 7.57 (d, *J* = 8.4, 2H), 7.92 (d, *J* = 8.8, 2H), 7.98 (d, *J* = 16.0, 1H). MS (ESI): 429.50 (C<sub>28</sub>H<sub>28</sub>O<sub>4</sub>, [M+H]<sup>+</sup>). Anal. Calcd for C<sub>28</sub>H<sub>28</sub>O<sub>4</sub>: C, 78.48; H, 6.59. Found: C, 78.24; H, 6.62.

**4.4.20. (E)-1-(4-Aminophenyl)-3-(2,4-dimethoxy-6-((E)-4-methoxystyryl)phenyl)prop-2-en-1-one (C20)**

Yellow solid (0.370 g, 89% yield). Mp 198–200 °C. <sup>1</sup>H NMR (400 MHz, CDCl<sub>3</sub>) δ (ppm): 3.86 (s, 3H), 3.92 (s, 6H), 4.11 (s, 2H), 6.27 (s, 1H), 6.64 (d, *J* = 8.4, 2H), 6.76 (s, 1H), 6.91 (d, *J* = 8.4, 2H), 6.97 (d, *J* = 16.0, 1H), 7.38 (d, *J* = 16.0, 1H), 7.49 (d, *J* = 8.4, 2H), 7.55 (d, *J* = 16.0, 1H), 7.89 (d, *J* = 8.4, 2H), 8.15 (d, *J* = 16.0, 1H). MS (ESI): 416.18 (C<sub>26</sub>H<sub>25</sub>NO<sub>4</sub>, [M+H]<sup>+</sup>). Anal. Calcd for C<sub>26</sub>H<sub>25</sub>NO<sub>4</sub>: C, 75.16; H, 6.06; N, 3.37. Found: C, 74.99; H, 6.08; N, 3.38.

**4.4.21. (E)-1-(4-(Diethylamino)phenyl)-3-(2,4-dimethoxy-6-((E)-4-methoxystyryl)phenyl)prop-2-en-1-one (C21)**

Yellow solid (0.434 g, 92% yield). Mp 148–150 °C. <sup>1</sup>H NMR (400 MHz, CDCl<sub>3</sub>) δ (ppm): 1.22 (t, *J* = 7.2, 6H), 3.44 (q, *J*<sub>1</sub> = 7.2, *J*<sub>2</sub> = 14.4, 4H), 3.86 (s, 3H), 3.92 (s, 6H), 4.11 (s, 2H), 6.46 (s, 1H), 6.65 (d, *J* = 8.4, 2H), 6.76 (s, 1H), 6.91 (d, *J* = 8.4, 2H), 7.14 (d, *J* = 16.0, 1H), 7.40 (d, *J* = 16.0, 1H), 7.50 (d, *J* = 8.4, 2H), 7.57 (d, *J* = 16.0, 1H), 7.95 (d, *J* = 8.4, 2H), 8.13 (d, *J* = 16.0, 1H). MS (ESI): 472.24 (C<sub>30</sub>H<sub>33</sub>NO<sub>4</sub>, [M+H]<sup>+</sup>). Anal. Calcd for C<sub>30</sub>H<sub>33</sub>NO<sub>4</sub>: C, 76.41; H, 7.05; N, 2.97. Found: C, 76.22; H, 7.07; N, 2.87.

**4.4.22. (E)-1-([1,1'-Biphenyl]-4-yl)-3-(2,4-dimethoxy-6-((E)-4-methoxystyryl)phenyl)prop-2-en-1-one (C22)**

Yellow solid (0.405 g, 85% yield). Mp 173–175 °C. <sup>1</sup>H NMR (400 MHz, CDCl<sub>3</sub>) δ (ppm): 3.86 (s, 3H), 3.93 (s, 6H), 6.47 (s, 1H), 6.76 (s, 1H), 6.92 (d, *J* = 8.0, 4H), 6.97 (d, *J* = 16.0, 1H), 7.26 (d, *J* = 8.0, 2H), 7.43–7.51 (dd, 3H), 7.37 (d, *J* = 16.0, 1H), 7.49 (d, *J* = 8.0, 2H), 7.58 (d, *J* = 16.0, 1H), 8.01 (d, *J* = 8.0, 2H), 8.18 (d, *J* = 16.0, 1H). MS (ESI): 477.20 (C<sub>32</sub>H<sub>28</sub>O<sub>4</sub>, [M+H]<sup>+</sup>). Anal. Calcd for C<sub>32</sub>H<sub>28</sub>O<sub>4</sub>: C, 80.65; H, 5.92. Found: C, 80.35; H, 5.90.

**4.4.23. (E)-3-(2,4-Dimethoxy-6-((E)-4-methoxystyryl)phenyl)-1-(4-morpholinophenyl)prop-2-en-1-one (C23)**

Yellow solid (0.461 g, 95% yield). Mp 167–169 °C. <sup>1</sup>H NMR (400 MHz, CDCl<sub>3</sub>) δ (ppm): 3.33 (t, *J* = 4.8, 4H), 3.86 (s, 3H), 3.90

(t, *J* = 4.8, 4H), 3.93 (s, 6H), 6.49 (s, 1H), 6.76 (s, 1H), 6.92 (d, *J* = 8.0, 4H), 6.97 (d, *J* = 16.0, 1H), 7.38 (d, *J* = 16.4, 1H), 7.50 (d, *J* = 8.4, 2H), 7.57 (d, *J* = 15.6, 1H), 7.98 (d, *J* = 8.4, 2H), 8.17 (d, *J* = 15.6, 1H). MS (ESI): 486.22 (C<sub>30</sub>H<sub>31</sub>NO<sub>5</sub>, [M+H]<sup>+</sup>). Anal. Calcd for C<sub>30</sub>H<sub>31</sub>NO<sub>5</sub>: C, 74.21; H, 6.43; N, 2.88. Found: C, 73.95; H, 6.45; N, 2.87.

**4.5. Antiproliferation assay**

The antiproliferative activity of the prepared compounds against HepG2, B16-F10, and A549 cell lines were evaluated as described elsewhere with some modifications.<sup>27</sup> Target tumor cell lines were grown to log phase in RPMI 1640 medium supplemented with 10% fetal bovine serum. After diluting to 2 × 10<sup>4</sup> cells mL<sup>-1</sup> with the complete medium, 100 μL of the obtained cell suspension was added to each well of 96-well culture plates. The subsequent incubation was permitted at 37 °C, 5% CO<sub>2</sub> atmosphere for 24 h before the cytotoxicity assessments. Tested samples at pre-set concentrations were added to six wells with colchicine and CA-4 coassayed as positive reference. After 48 h exposure period, 40 μL of PBS containing 2.5 mg mL<sup>-1</sup> of MTT (3-(4,5-dimethylthiazol-2-yl)-2,5-diphenyltetrazolium bromide) was added to each well. 4 h later, 100 μL extraction solution (10% SDS–5% isobutyl alcohol–0.01 M HCl) was added. After an overnight incubation at 37 °C, the optical density was measured at a wavelength of 570 nm on an ELISA microplate reader. In all experiments three replicate wells were used for each drug concentration. Each assay was carried out at least three times. The results were summarized in Table 1.

**4.6. Effects on tubulin polymerization**

Bovine brain tubulin was purified as described previously.<sup>28</sup> To evaluate the effect of the compounds on tubulin assembly *in vitro*,<sup>29</sup> varying concentrations were preincubated with 10 μM tubulin in glutamate buffer at 30 °C and then cooled to 0 °C. After addition of GTP, the mixtures were transferred to 0 °C cuvettes in a recording spectrophotometer and warmed up to 30 °C and the assembly of tubulin was observed turbidimetrically. The IC<sub>50</sub> was defined as the compound concentration that inhibited the extent of assembly by 50% after 20 min incubation.

**4.7. Docking simulations**

Molecular docking of compound **C19** into the three-dimensional X-ray structure of tubulin (PDB code: 1SA0) was carried out using the Auto-Dock software (version 4.0) as implemented through the graphic user interface Auto-Dock Tool Kit (ADT 1.4.6).<sup>30</sup>

The graphical user interface AUTODOCKTOOLS was employed to set-up the enzymes: all hydrogens were added, Gasteiger charges were calculated and nonpolar hydrogens were merged to carbon atoms. The Ni initial parameters are set as *r* = 1.170 Å, *q* = +2.0, and van der Waals well depth of 0.100 kcal/mol.<sup>31</sup> For macromolecules, generated pdbqt files were saved.

The 3D structures of ligand molecules were built, optimized (PM3) level, and saved in Mol2 format with the aid of the molecular modeling program SPARTAN (Wavefunction Inc.). These partial charges of Mol2 files were further modified by using the ADT package (version 1.4.6) so that the charges of the nonpolar hydrogens atoms assigned to the atom to which the hydrogen is attached. The resulting files were saved as pdbqt files.

AUTODOCK 4.0 was employed for all docking calculations. The AUTODOCKTOOLS program was used to generate the docking input files. In all docking a grid box size of 60 × 60 × 60 points in *x*, *y*, and *z* directions was built, the maps were centered on N1 atom of the

Kcx 219 in the catalytic site of the protein. A grid spacing of 0.375 Å (approximately one fourth of the length of carbon–carbon covalent bond) and a distances-dependent function of the dielectric constant were used for the calculation of the energetic map. Ten runs were generated by using Lamarckian genetic algorithm searches. Default settings were used with an initial population of 50 randomly placed individuals, a maximum number of  $2.5 \times 10^6$  energy evaluations, and a maximum number of  $2.7 \times 10^4$  generations. A mutation rate of 0.02 and a crossover rate of 0.8 were chosen. Results differing by less than 0.5 Å in positional root-mean-square deviation (RMSD) were clustered together and the results of the most favorable free energy of binding were selected as the resultant complex structures.

### Acknowledgments

This work was supported by the Jiangsu National Science Foundation (No. BK2009239) and Jiangsu Postdoctoral Science Foundation (No. 1001006C).

### References and notes

- Aggarwal, B. B.; Bhardwaj, A.; Aggarwal, R. S.; Seeram, N. P.; Shishodia, S.; Takada, Y. *Anticancer Res.* **2004**, *24*, 2783.
- Jang, M.; Cai, L.; Udeani, G. O.; Slowing, K. V.; Thomas, C. F.; Beecher, C. W.; Fong, H. H.; Farnsworth, N. R.; Kinghorn, A. D.; Mehta, R. G.; Moon, R. C.; Pezzuto, J. M. *Science* **1997**, *275*, 218.
- Signorelli, P.; Ghidoni, R. J. *Nutr. Biochem.* **2005**, *16*, 449.
- Murias, M.; Handler, N.; Erker, T.; Pleban, K.; Ecker, G.; Saiko, P.; Szekeres, T.; Jager, W. *Bioorg. Med. Chem.* **2004**, *12*, 5571.
- Xu, G. L.; Liu, F.; Ao, G. Z.; He, S. Y.; Ju, M.; Zhao, Y.; Xue, T. *Eur. J. Pharmacol.* **2009**, *611*, 100.
- Kumar, A.; Sharma, S. S. *Biochem. Biophys. Res. Commun.* **2010**, *394*, 360.
- Buryanovskyy, L.; Fu, Y.; Boyd, M.; Ma, Y. L.; Hsieh, T. C.; Wu, J. M.; Zhang, Z. T. *Biochemistry* **2004**, *43*, 11417.
- Sun, B.; Hoshino, J.; Jermihov, K.; Marler, L.; Pezzuto, J. M.; Mesecar, A. D.; Cushman, M. *Bioorg. Med. Chem.* **2010**, *18*, 5352.
- Ulrich, S.; Huwiler, A.; Loitsch, S.; Schmidt, H.; Stein, J. M. *Biochem. Pharmacol.* **2007**, *74*, 281.
- Wang, Y.; Leung, L. K. *Toxicol. Lett.* **2007**, *173*, 175.
- Park, E. J.; Park, H. R.; Lee, J. S.; Kim, J. *Planta Med.* **1998**, *64*, 464.
- Claude, A. C.; Jean, C. L.; Patric, T.; Christelle, P.; Gerard, H.; Albert, J. C.; Jean, L. D. *Anticancer Res.* **2001**, *21*, 3949.
- Kumar, S. K.; Erin, H.; Catherine, P.; Halluru, G.; Davidson, N. E.; Khan, S. R. J. *Med. Chem.* **2003**, *46*, 2813.
- Ko, H. H.; Tsao, L. T.; Yu, K. L.; Liu, C. T.; Wang, J. P.; Lin, C. N. *Bioorg. Med. Chem.* **2003**, *11*, 105.
- Matsuda, H.; Morikawa, T.; Ando, S.; Iwao, T.; Mas-ayuki, Y. *Bioorg. Med. Chem.* **2003**, *11*, 1995.
- Parmar, V. S.; Sharma, N. K.; Husain, M.; Watterson, A. C.; Kumar, J.; Samuelson, L. A.; Ashok, L. C.; Prasad, A. K.; Kumar, A.; Malhotra, S.; Kumar, N.; Jha, A.; Singh, A.; Singh, I.; Himanshu; Vats, A.; Shakil, N. A.; Trikha, S.; Mukherjee, S.; Sharma, S. K.; Singh, S. K.; Kumar, A.; Jha, H. N.; Olsen, C. E.; Stove, C. P.; Bracke, M. E.; Mareel, M. M. *Bioorg. Med. Chem.* **2003**, *11*, 913.
- Qian, Y.; Ma, G. Y.; Yang, Y.; Cheng, K.; Zheng, Q. Z.; Mao, W. J.; Shi, L.; Zhao, J.; Zhu, H. L. *Bioorg. Med. Chem.* **2010**, *18*, 4310.
- Lahtchev, K. L.; Batovska, D. I.; Parushev, St. P.; Ubiyvovk, V. M.; Sibirny, A. A. *Eur. J. Med. Chem.* **2008**, *43*, 2220.
- Dimmock, J. R.; Elias, D. W.; Beazely, M. A.; Kandepu, N. M. *Curr. Med. Chem.* **1999**, *6*, 1125.
- McGrogan, B. T.; Gilmartin, B.; Carney, D. N.; McCann, A. *Biochim. Biophys. Acta* **2008**, *1785*, 96.
- Pascal, V. P.; Garès, M.; Michel, W. *Biochem. Pharmacol.* **1999**, *59*, 959.
- Young, S. L.; Chaplin, D. J. *Expert Opin. Invest. Drugs* **2004**, *13*, 1171.
- Hu, L. X.; Li, Z. R.; Li, Y.; Qu, J. R.; Ling, Y. H.; Jiang, J. D.; Boykin, D. W. *J. Med. Chem.* **2006**, *49*, 6273.
- Huang, X. F.; Ruan, B. F.; Wang, X. T.; Xu, C.; Ge, H. M.; Zhu, H. L.; Tan, R. X. *Eur. J. Med. Chem.* **2007**, *42*, 263.
- Huang, X. F.; Shi, L.; Li, H. Q.; Zhu, H. L. *J. Chem. Crystallogr.* **2007**, *3*, 739.
- Julio, M. V.; Sylvia, P. D. C.; Josefina, S. F.; Francisco, D. V.; Rivero, I. A. *Bioorg. Med. Chem.* **2009**, *17*, 6780.
- Boumendjel, A.; Boccard, J.; Carrupt, P.-A.; Nicolle, E.; Blanc, M.; Geze, A.; Choïnard, L.; Wouessidjewe, D.; Matera, E.-L.; Dumontet, C. *J. Med. Chem.* **2008**, *51*, 2307.
- Hamel, E.; Lin, C. M. *Biochemistry* **1984**, *23*, 4173.
- Hamel, E. *Cell Biochem. Biophys.* **2003**, *38*, 1.
- Huey, R.; Morris, G. M.; Olson, A. J.; Goodsell, D. S. *J. Comput. Chem.* **2007**, *28*, 1145.
- Musiani, F.; Arnofi, E.; Casadio, R.; Ciurli, S. *J. Biol. Inorg. Chem.* **2001**, *6*, 300.